J. Biochem. **134**, 333–344 (2003)
DOI: 10.1093/jb/mvg150

Two Mitofusin Proteins, Mammalian Homologues of FZO, with Distinct Functions Are Both Required for Mitochondrial Fusion

Yuka Eura[*,1], Naotada Ishihara[*,1], Sadaki Yokota[2] and Katsuyoshi Mihara[†,1]

[1]Department of Molecular Biology, Graduate School of Medical Science, Kyushu University, Fukuoka 812-8582; and [2]Biological Program, Yamanashi Medical University, Yamanashi, 409-3898

Received April 15, 2003; accepted June 9, 2003

Mitochondria are dynamic organelles that undergo frequent fission and fusion or branching. Although these morphologic changes are considered crucial for cellular functions, the underlying mechanisms remain elusive, especially in mammalian cells. We characterized two rat mitochondrial outer membrane proteins, Mfn1 and Mfn2, with distinct tissue expressions, that are homologous to *Drosophila* Fzo, a GTPase involved in mitochondrial fusion. Expression of the GTPase-domain mutant of Mfn2 (Mfn2^{K109T}) in HeLa cells induced mitochondrial fragmentation in which Mfn2^{K109T} localized at the restricted domains. Immuno-electronmicroscopy revealed that Mfn2^{K109T} was concentrated at the contact domains between adjacent mitochondria, suggesting that fusion of the outer membrane was arrested at some intermediate step. Mfn1 expression induced highly connected tubular network structures depending on the functional GTPase domain. The Mfn1-induced tubular networks were suppressed by co-expression with Mfn2. *In vivo* depletion of either isoform by RNA interference revealed that both are required to maintain normal mitochondrial morphology. The fusion of differentially-labeled mitochondria in HeLa cells subjected to depletion of either Mfn isoform and subsequent cell fusion by hemagglutinating virus of Japan revealed that both proteins have distinct functions in mitochondrial fusion. We conclude that the two Mfn isoforms cooperate in mitochondrial fusion in mammalian cells.

Key words: GTPase, mitochondria, membrane fusion, organelle morphology, RNAi.

Abbreviations: Mfn1^{K88T} and Mfn2^{K109T}, the GTPase domain mutants of Mfn1 and Mfn2, respectively; HA, hemagglutinin; HVJ, Hemagglutinating Virus of Japan; RNAi, RNA interference; siRNA, small interference RNA; WT, wild-type.

Mitochondria are very dynamic, changing their size, shape, position, or copy number in cells during cellular differentiation, development, or under pathologic conditions (*1–3*). The inheritance of mitochondria or maintenance of their characteristic shape and position is regulated by fusion and fission reactions and by active transport along cytoskeletal elements, such as actin, microtubule, or intermediate filaments (*2*, *4*).

Recent studies in yeast revealed that three high molecular-weight GTP-binding proteins are involved in mitochondrial morphogenesis (*2*, *5*, *6*). A soluble dynamin-related GTPase, Dnm1, assembles on the mitochondrial outer membrane and mediates mitochondrial division; *dnm1* mutations produce long tubular mitochondria or those with a planar net of interconnected tubules (*7*, *8*). Mutations in the second dynamin family protein, Mgm1, cause mitochondrial aggregation and mitochondrial DNA loss (*9–11*). Mgm1 is thought to regulate inner membrane remodeling in the intermembrane space (*11–13*). A GTP-binding transmembrane protein, *fuzzy onion* (Fzo), in *Drosophila* and a yeast homologue, Fzo1, function in the mitochondrial membrane fusion reaction (*14–16*). In *Drosophila*, Fzo is expressed specifically in testis at a restricted stage during spermatogenesis and is required for a developmentally-regulated mitochondrial fusion event (*14*). In yeast *S. cerevisiae*, a conditional *fzo1* mutation induces fragmentation of the mitochondrial reticulum and blocks mitochondrial fusion during yeast mating (*15*, *16*). Fzo1 is anchored to the outer membrane by two adjacent transmembrane segments at the C-terminus, exposing both the bulk N-terminal portion and a small C-terminal segment to the cytosol (*17*). A short loop connecting the two transmembrane segments exposed to the intermembrane space associates with the inner membrane and this association is critical for its function (*17*).

Much less is known about the mechanisms that regulate mitochondrial morphology in mammalian cells. A cytosolic dynamin-like protein (Dlp1 or Drp1) functions as an orthologue of yeast Dnm1 in the mitochondrial fission process in mammalian cells (*18–21*). Expression of the GTPase-domain mutant in cultured cells causes a collapse of the mitochondrial network to large perinuclear aggregates, or mitochondrial enlargement (*22–25*). Drp1 is also involved in apoptotic cell death. Upon the induction of apoptosis, Drp1 translocates from the cytosol to the potential division sites of mitochondria to induce mitochondrial fragmentation (*26*). Recent research has revealed that mutations in the human *OPA1* gene, which encodes a protein structurally similar to yeast Mgm1,

[*]These authors contributed equally to this work.
[†]To whom correspondence should be addressed. Tel: +81-92-642-6176, Fax: +81-92-642-6183, E-mail: mihara@cell.med.kyushu-u.ac.jp

induce optic atrophy through mitochondrial impairment (*27*, *28*). Santel and Fuller (2001) identified two human homologues of Fzo, mitofusin1 and 2 (Mfn1 and Mfn2). The expression of either protein in cultured mammalian cells induces mitochondrial clustering (*29*). Rojo *et al*. (2002) reported that the exogenously expressed Mfn2 localizes on the contact region of connected mitochondria (*30*). Co-expression of Mfn2 with a dominant negative GTPase mutant of Drp1 that blocks mitochondrial fission results in elongation of the mitochondrial filaments and networks, suggesting that mitochondrial morphogenesis depends on a dynamic balance between Mfn-dependent mitochondrial fusion and Drp1-dependent mitochondrial fission (*29*). Whether these two Mfn isoforms have functional redundancy or function in distinct steps, however, remains unknown.

For the present report, we characterized rat Mfn1 and Mfn2, proteins that exhibit distinct tissue expression patterns. Expression of the GTPase-negative mutant of Mfn2 ($Mfn2^{K109T}$) in cultured cells and examination of the cells by immunofluorescent microscopy and immunoelectronmicroscopy revealed $Mfn2^{K109T}$-induced mitochondrial fragmentation and the accumulation of an apparent intermediate of the mitochondrial fusion process. Expression of wild-type Mfn1 induced protrusion of highly connected network structures, possibly derived from the outer membrane. The network structures collapsed to the normal structure upon co-expression with Mfn2, indicating the cooperation of both isozymes in mitochondrial morphogenesis. The involvement of both isoforms in a distinct step of the fusion reactions was verified by examining morphologic changes in mitochondria induced by the depletion of either isoform using RNA interference (RNAi), or by mitochondrial fusion assay using hemagglutinating virus of Japan (HVJ)-induced cell fusion in conjunction with RNAi. We conclude that the two mitofusin proteins function in mitochondrial outer membrane fusion reactions in a cooperative manner.

MATERIALS AND METHODS

Materials—The rat liver cDNA library in λgt10 was described previously (*31*). The rabbit polyclonal antibodies against rat Tom40 (*32*), rat Tom70 (*33*), rat Tim17, and rat Tim44 (*34*) were described previously. The rabbit polyclonal antibodies against HA (BAbCO), and the monoclonal antibodies against HA (16B12; BAbCO) and FLAG (M2; Sigma Chemical, St. Louis, MO) were purchased from the indicated companies. Expression plasmids of rat Tom22 (*35*) and HVJ (*36*) for cell fusion were gifts from Y. Nakamura (Kyushu University) and Y. Yoneda (Osaka University), respectively.

cDNA Cloning of Rat Mitofusin Proteins—The following oligonucleotides were synthesized based on the cDNA sequence of KIAA0214 for Mfn2, or mouse ESTs for Mfn1, AN1: 5′-GCCGGGAAGGTGAAGTTC-3′, AC1: 5′-TGAGCTGACCAGTCCTTG-3′, BN1: 5′-ATAATGGCAGAAACGGTATCTC-3′, BC1: 5′-TTAGGATTCTCCACTGCTCGGGTG-3′. The 2,613-bp fragment of rat Mfn2 and the 2,229-bp fragment of rat Mfn1 were amplified from rat liver poly(A)-RNA by RT-PCR using AN1 and AC1 for Mfn2, and BN1 and BC1 for Mfn1. The fragments were subcloned into the pGEM-T easy vector (Promega). To obtain a full-size rat Mfn1 cDNA, a λgt10 rat liver cDNA library was screened using the PCR fragment as the probe. Sequence data are available from GenBank/EMBL/DDB under accession no. AB084165 (rat Mfn2) and AB084166 (rat Mfn1).

Preparation of Antibodies against Rat Mitofusin Proteins—The *Bam*HI–*Hin*dIII fragments of rat Mfn2 and the C-terminal-truncated form of Mfn1 (Mfn1ΔC) were amplified by PCR using the primer AN-*Bam*HI: 5′-CTCGGATCCATGTCCCTGCTCTTTTC-3′ and AC-*Hin*dIII: 5′-ATTAAGCTTCTATCTGCTGGGCTG-3′ for Mfn2, or BN-*Bam*HI: 5′-CTCGGATCCATGGCAGAAACGGTATC-3′ and BC-*Hin*dIII: 5′-CTCAAGCTTCTACTCTTCCTGGGCTGC-3′ for Mfn1, and subcloned into the pET28a vector (Novagen). BL21 (DE3) cells harboring the plasmids were cultured at 37°C (for Mfn2) or at 30°C (for Mfn1) in 1 mM IPTG for 5 h. The N-terminal His6-tagged proteins expressed as inclusion bodies were subjected to SDS-PAGE, eluted from the gel, and used to raise antibodies in rabbits. Specific IgGs recognizing only Mfn2 or Mfn1 were isolated as follows. The IgGs against Mfn1 were selected using Mfn1-conjugated Formyl Cellulofine beads (Seikagaku Kogyo, Japan) followed by removal of the IgGs that recognized Mfn2 using Mfn2-conjugated beads, or *vice versa*.

Construction of Mammalian Expression Plasmids—The PCR fragments of rat Mfn2 and Mfn1 were amplified using primers. AN-*Hin*dIII: 5′-ATGCAAGCTTCCACCATGTCCCTG-3′, and AC-*Bln*I: 5′-ATTCCTAGGTCTGCTGGGCTGCAGGTAC-3′ for Mfn2, or BN-*Hin*dIII: 5′-ATGCAAGCTTCCACCATGGCAGAAACGGTATCTC-3′ and BC-*Bln*I: 5′-ATACCTAGGGGATTCTCCACTGCTCGGGT-3′ for Mfn1 (*Hin*dIII and *Bln*I sites are underlined), and subcloned into pRcCMV-HA to create the expression plasmids for the C-terminal HA-tagged Mfn proteins (*37*). Point mutations in the G1 motif of the GTPase domain were introduced by changing; 109K in Mfn2 to 109T, or 88K in Mfn1 to 88T using the primers AG1-KT: 5′-ATTGATCACGGTACTAGTCCCATTGCTCGT-3′ for Mfn2, or BG1-KT: 5′-GTTGATGACAGAACTAGTGCCACTACTTGT-3′ for *M*fn1 (*Spe*I sites are underlined). The C-terminal FLAG-tagged Mfn proteins were constructed as follows. The PCR fragments were amplified by AN-*Bam*HI-FLAG: 5′-ACTGGGATCCCCACCATGTCCCTGCTCTTT-3′ and AC-*Bam*HI-FLAG: 5′-TCAGTGGATCCTCTGCTGGGCTGCAGGTAC-3′ for Mfn2, and BN-*Hin*dIII and BC-*Bln*I for Mfn1. These fragments were subcloned into p3xFLAG-CMV-14 (Sigma Chemical). For the construction of mitochondria-targeted green fluorescent protein (GFP) or DsRed red fluorescent protein (RFP), the mitochondrial targeting signal (residues 1–69) of the precursor of *N. crassa* F0 ATPase subunit 9 (*38*) was amplified by PCR using the following primers and pSu9(*1*–69)-DHFR as the template. Eco-Su9: 5′-ACTAGAATTCATGGCCTCCACTCGTGTCC-3′ Bam-Su9: 5′-TCATGGATCCGAAGAGTAGGCGCGCTTC-3′ The obtained fragment was subcloned into pEGFP-N1 or pDsRed1-N1 vectors (Clontech).

Immunofluorescence Microscopy—HeLa cells were cultured on coverslips in 35-mm dishes in 2 ml Dulbecco's modified Eagle's medium supplemented with 10% fetal calf serum (FCS) at 37°C overnight under an atmosphere

of 5% CO_2. Transfection was performed using Lipofectamine (Lifetech). The cells were incubated for 18 h and then stained with 20 nM of MitoTracker Red CMXRos (Molecular Probes) before fixation. The cells on the coverslips were fixed with 50% acetone-50% methanol for 2 min at room temperature, and then indirect immunofluorescence staining was performed as described previously (*39*) using fluorescein isothiocyanate (FITC)-conjugated goat antibodies against rabbit IgG, Texas Red-conjugated goat antibodies against rabbit IgG, FITC-conjugated goat antibodies against mouse IgG (BioSOURCE), or Cy5-conjugated goat antibodies against mouse IgG (Amersham/ Pharmacia). Fluorescent images were analyzed using a confocal laser microscope (Radiance 2000, Bio-Rad).

Electron Microscopy—Transfected HeLa cells were cultured for 18 h and fixed for 30 min at room temperature with 4% paraformaldehyde and 0.25% glutaraldehyde in 0.2 M Hepes-KOH buffer (pH 7.4). The cells were washed with phosphate buffered saline, briefly stained with 0.02% toluidine blue, detached from the culture dishes with a rubber policeman in the presence of 20% ethanol, and collected by centrifugation. Cell pellets were then suspended in 1% low-melting temperature agarose, centrifuged, and quenched in a refrigerator. The agarose-cell pellets were cut into small pieces, some of which were dehydrated in a graded ethanol series at –20°C and embedded in LR White (*40*). Others were fixed in 1% reduced osmium for 1 h at room temperature, dehydrated, and embedded in Epon 812. For immuno-electron microscopy, LR White-embedded cells were cut into thin sections with a diamond knife using a Reichert Ultracut R (Leica) and mounted on nickel. Sections were treated with 0.5% bovine serum albumin solution for 10 min and then with primary antibody overnight at 4°C. The sections were subjected to rigorous washing with phosphate buffered saline, and then incubated with Protein A-gold (15 nm in diameter) for 30 min at room temperature. After washing with distilled water, sections were stained with 2% uranyl acetate for 8 min and with lead citrate for 30 s. For routine electron microscopy, Epon-embedded cells were cut into thin sections, mounted on copper grids, and stained with lead citrate. All sections were observed with a Hitachi H7500 electron microscope at an 80-kV acceleration voltage.

Immunoprecipitation—The HeLa cells expressing Mfn1, Mfn2, or both were lysed in the lysis buffer: 50 mM Tris-HCl (pH 7.5) containing 150 mM NaCl, 1 mM $MgCl_2$, 0.5 mM phenylmethylsulfonyl fluoride, 10 μg/ml α2-macroglobulin, protease inhibitor cocktail, 1% digitonin, in the absence or presence of 2 mM GTP or GTPγS. The lysates were cleared by centrifugation two times at 12000 rpm for 5 min in a microfuge, and the supernatant fractions were subjected to immunoprecipitation using polyclonal anti-HA antibodies and Protein A-Sepharose. The precipitates were analyzed by SDS-PAGE and subsequent immunoblotting using monoclonal anti-HA, anti-FLAG, or polyclonal anti-Tom40 antibodies. Band intensity was quantified using the Image Gauge program (Fuji, Tokyo).

RNAi—For RNAi assay, 21 nucleotide small interference RNAs (siRNAs) comprising 19 nucleotides and a dTdT overhang at each 3′-terminus were chemically synthesized (*41*). The synthesized siRNAs corresponded to the 1973–1991 coding region of Mfn2 (RNAiAC-1 and RNAiAC-2) and the 1150–1168 region of Mfn1 (RNAiB-1 and RNAiB-2), regions that are completely conserved between rats and humans. RNAiAC-1: 5′-AGAGGGCCUUCAAGCGCCATT-3′, RNAiAC-2: 5′-UGGCGCUUGAAGGCCCUCUTT-3′, RNAiB-1: 5′-CGAAACCAGAUGAACCUUUTT-3′, RNAiB-2: 5′-AAAGGUUCAUCUGGUUUCGTT-3′

HeLa cells in 35-mm dishes were transfected two times at a 24-h interval with the annealed siRNA duplex (1.4 μg) using Oligofectoamine (Lifetech) and cultured further for 24 h.

HVJ-Induced Cell Fusion and Assay for Mitochondrial Fusion—HeLa cells transfected with the Su9GFP or Su9RFP expression vectors were co-cultured in a glass-base dish. The cells were fused by HVJ as described previously (*36*). Briefly, the dish was washed three times with ice-cold BSS-Ca (10 mM Tris-HCl, pH 7.4, 140 mM NaCl and 2 mM CaCl2), then incubated on ice with BSS-Ca containing HVJ for 30 min. The dish was washed two times with BSS-Ca, the medium was changed to Dulbecco's modified Eagle's medium with 10% FCS, and the cells were cultured at 37°C. The heterokaryons made from Su9GFP- and Su9RFP-expressing cells were analyzed by confocal microscopy (*42*). To analyze mitochondrial fusion in cells subjected to RNAi, the siRNA-transfected cells described above were transfected separately with Su9GFP or Su9RFP, cultured for 24 h after the last siRNA transfection, and then subjected to the cell fusion reaction. The colocalization frequency of GFP- and RFP-labeled mitochondrial signals in the fused cells was quantified using MetaMorph software (Roper).

RESULTS

Isolation of Rat Mitofusin cDNAs—Drosophila Fzo and yeast Fzo1 are involved in mitochondrial fusion reactions (*14–16*). To investigate the molecular mechanism of mammalian mitochondrial morphogenesis, we isolated rat homologues of Fzo. Two cDNAs were isolated from rat liver. One cDNA encoded a protein of 753 amino acid residues (86.1 kDa), and the other encoded a protein of 741 amino acid residues (84.0 kDa). These two proteins shared 63% overall sequence identity, and 32% and 31% identity with *Drosophila* Fzo, respectively. Both proteins showed 12% identity with yeast Fzo1.

Sequence comparisons revealed that the 86.1-kDa protein and 84.0-kDa protein are the rat counterparts of human Mfn2 (95% identity) and Mfn1 (90% identity), respectively (*29*).

Two rat Mfn Proteins Exhibit Distinct Tissue Expression Patterns—Immunoblot analyses of rat liver subcellular and submitochondrial fractions with isoform-specific antibodies (Fig. 1A) revealed that Mfn proteins localize in the mitochondrial outer membranes with the bulk N-terminal portion extruding into the cytosol (data not shown). Immunoblot analysis with these antibodies also showed these Mfn proteins to be expressed in all tissues examined, although with differing protein expression levels (Fig. 1B). Both isoforms are expressed at comparable levels in liver, kidney, and adrenal glands. In the brain, *Mfn*2 is expressed predominantly, and Mfn1 only margin-

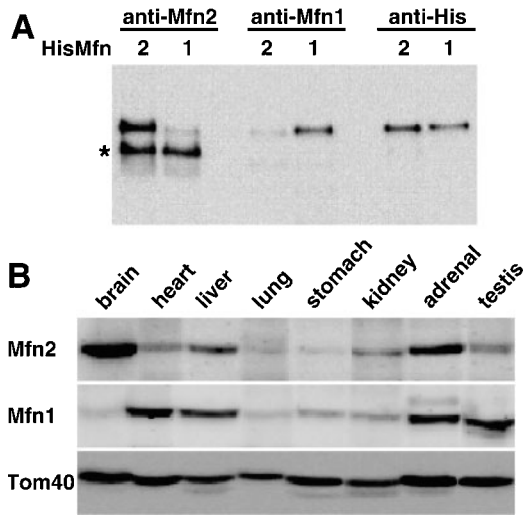

Fig. 1. **Tissue expression of rat Mfn proteins.** (A) Specificity of anti-rat Mfn antibodies. Recombinant His-Mfn2 and His-Mfn1 proteins were analyzed by immunoblotting using the indicated antibodies. A nonspecific band detected by anti-Mfn2 IgGs is indicated by an asterisk. (B) The total proteins (20 μg each) prepared from the indicated tissues of adult rat were subjected to immunoblotting using anti- rat Mfn1, rat Mfn2, or rat Tom40 antibodies.

ally. Conversely, in heart and testis, Mfn1 is highly expressed compared with Mfn2. As a control, Tom40 was found to be expressed to a similar extent in all tissues examined. There is general tissue expression of both Mfn isozymes at the mRNA level in rats (Ishihara *et al.*, unpublished results) humans, and mice (*30*). The relative amounts of the two isoforms might influence mitochondrial morphology and function in different tissues.

Expression of Two Mfn Proteins and Their GTPase Domain Mutants Induces Distinct Mitochondrial Morphologic Changes—There are several reports on exogenous Mfn1 and Mfn2 expression in cultured mammalian cells. The expression of human Mfn2 and its GTPase domain mutant in mammalian cultured cells induces perinuclear clustering of mitochondria, bringing mitochondrial membranes into close contact (*29*). Mfn2 localizes at the contact regions of mitochondria (*30*). On the other hand, Mfn1 expression activates the mitochondrial filamentous structure (*43*). The functional difference between the two Mfn proteins in mitochondrial morphogenesis, however, remains unknown. To address this, rat Mfn proteins HA-tagged at the C-termini were expressed in HeLa cells, and their intracellular localizations and mitochondrial morphologic changes were examined using indirect immunofluorescence microscopy with anti-HA antibodies.

The exogenously expressed Mfn isoforms or their mutants were expressed to a comparable extent and recovered in the membrane fraction in a Triton X-100-extractable form (Fig. 2, B and C), indicating that they were not in the form of protein aggregates, but instead were inserted correctly into the mitochondrial membrane. When Mfn2 was expressed in HeLa cells, it colocalized with MitoTracker, a mitochondria-specific dye ("wt" in Fig. 2A), or the mitochondrial outer membrane protein Tom70 (data not shown). In cells expressing lower levels of Mfn2, mitochondrial networks were slightly exaggerated compared with those in untransfected cells (Fig. 2A, a–c; compare with nontransfected cells in the same field). In contrast, in cells showing strong Mfn2 immunofluorescent signals, thick mitochondrial aggregation was induced in the perinuclear regions and the expressed Mfn2 localized to the aggregated mitochondria with a small fraction mistargeted to the cytoplasm (Fig. 2A; d–f). Of expressing cells, ~40% had aggregated mitochondria similar to panels d–f in Fig. 2A, and ~50% had filamentous mitochondria, similar to panels a–c in Fig. 2A (Fig. 2D). The expression of human Mfn1 and Mfn2 induces similar perinuclear mitochondrial aggregates in COS cells (*29*). Such mitochondrial aggregations were also observed in most COS cells expressing rat Mfn proteins or their mutants (data not shown). This is probably because the efficiency of protein expression in COS cells is higher than that in HeLa cells. Similar morphologic changes were also frequently observed in cells overexpressing mitochondrial outer membrane proteins, such as Tom20 (*44*, *45*) and OM37 (Maeda *et al.*, unpublished observations). We conclude that moderate expression of Mfn2 only slightly stimulates mitochondrial network formation.

When Mfn1 was expressed at lower levels in HeLa cells, some fraction of the expressed Mfn1 was concentrated in subdomains of mitochondria as punctate structures, although the remainder was distributed in normal-shaped mitochondrial networks (Fig. 2A, m–o). In cells expressing Mfn1 at higher levels, perinuclear aggregation of mitochondria was induced, and surprisingly, there were highly elongated and connected tubulo-network structures extending from the aggregated mitochondria toward the cell peripheri (Fig. 2A, p–r, see also Fig. 4A). These structures were not detectable in control cells or in cells expressing Mfn2 (Fig. 2D). The frequency of normal-shaped mitochondria decreased to 24% of the expressed cells, and 30% of cells showed tubulo-network structures (Fig. 2D). Thus, the expression of two rat Mfn isoforms induced clearly distinct changes in mitochondrial morphology and distribution.

To probe the function of the GTPase domain of Mfn, we introduced a missense mutation in the G1 motif of the GTPase domain of Mfn2 (K109T; $Mfn2^{K109T}$) and Mfn1 (K88T; $Mfn1^{K88T}$). The G1 domain is required for nucleotide binding of GTPase proteins and these mutations inactivate *Drosophila* Fzo function (*14*). The $Mfn2^{K109T}$ mutation clearly altered both the localization of Mfn2 and mitochondrial morphology. In 36% of cells expressing $Mfn2^{K109T}$, the mitochondrial networks collapsed to form small and fragmented mitochondria, and the mutant protein accumulated in subdomains of the mitochondria as dot-like structures (Fig. 2A, g–i, and see magnified images in Fig. 3A, a–c). On the other hand, $Mfn1^{K88T}$ induced mitochondrial fragmentation to a weaker extent than $Mfn2^{K109T}$ (17%; similar to that of Mfn1-expressing cells), and the expressed protein colocalized with MitoTracker (Fig. 2A, s–u) or Tom70 (data not shown). Again, perinuclear mitochondrial clustering was observed in cells expressing higher levels of $Mfn1^{K88T}$ (Fig. 2A, v–x; ~50% of the expressed cells). In marked contrast to wild-type Mfn1, $Mfn1^{K88T}$ did not induce the characteristic tubulo-network structures, indicating the importance of the functional GTPase domain of Mfn1 for protrusion of

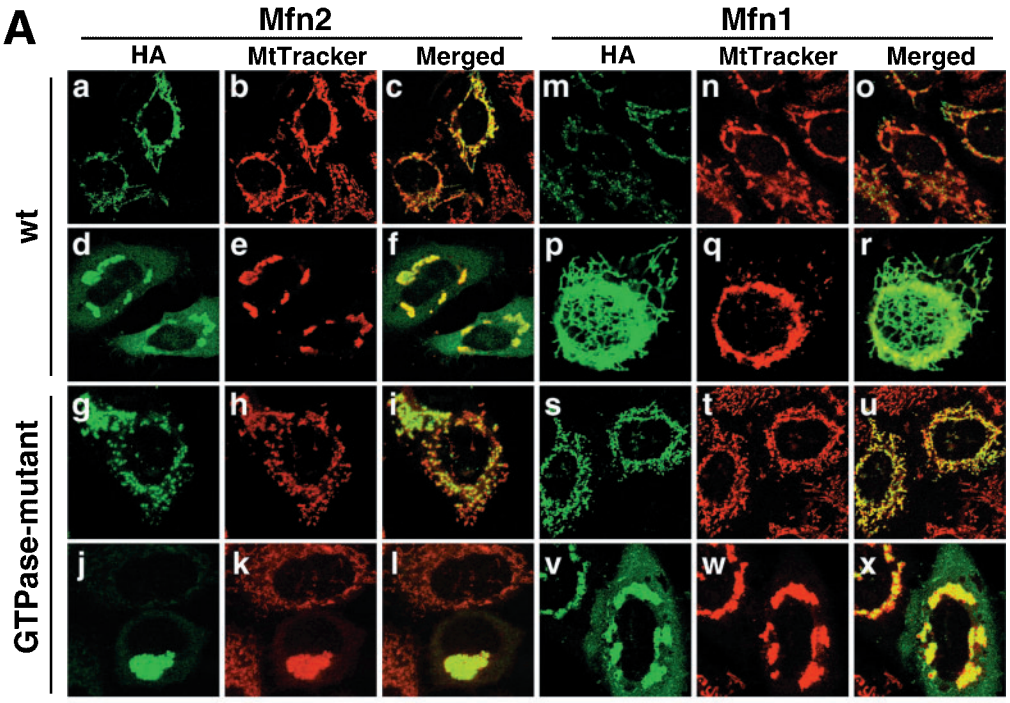

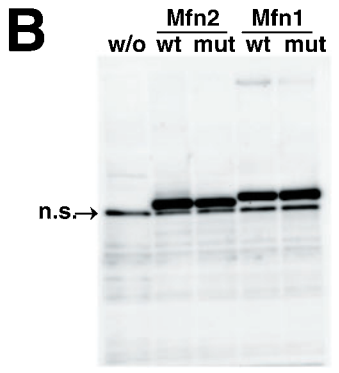

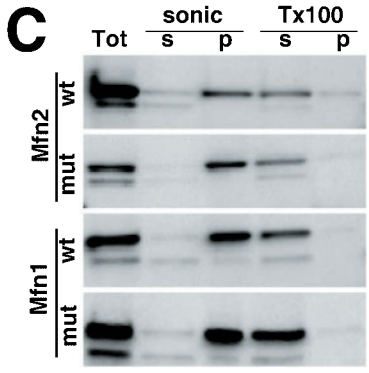

D

	normal	fragment	highly network	aggregate
w/o	83.3±0.5	8.0±2.2	0±0	9.0±1.4
Mfn2	54.3±0.5	3.3±0.9	0±0	42.3±1.2
Mfn1	24.3±5.4	16.3±6.2	30.3±8.2	29.0±7.8
Mfn2^{K109T}	8.7±2.1	36.0±6.2	0±0	55.3±8.2
Mfn1^{K88T}	34.7±3.9	17.0±3.7	0±0	48.3±5.3

Fig. 2. **Expression of the two isoforms of rat Mfn and their GTPase mutants in HeLa cells.** (A) Mfn2 (a–f), Mfn1 (m–r), Mfn2^{K109T} (g–l), and Mfn1^{K88T} (s–x), with HA at their C-termini, were transiently expressed in HeLa cells and cultured for 18 h. The cells were labeled with MitoTracker, and subjected to immunofluorescence microscopy using rabbit anti-HA antibodies. Images were obtained and analyzed by confocal laser-scanning microscopy. Typical images of each construct, selected from both moderate (top) and high expressing (bottom) cells, are shown. (B and C) Expression and membrane localization of Mfn proteins in HeLa cells. The constructs shown were transiently expressed in HeLa cells and cultured for 18 h. The cells were sonicated with or without Triton X-100 (Tx100) and centrifuged at 100k ×g to separate the supernatant (s) and pellet (p) fractions. Total cell extracts (B), or the s and p fractions (C) were subjected to immunoblotting using rabbit anti-HA antibodies. n.s., nonspecific bands in HeLa cells recognized by anti-HA antibodies. (D) Mitochondrial morphology in HeLa cells expressing rat Mfn isoforms or their GTPase mutants. The transfected HeLa cells were cultured for 18 h and the number of expressed cells with normal mitochondrial morphology ("normal"), fragmented mitochondria ("fragment"), filamentous network structures of Mfn ("highly network"), or mitochondrial aggregation ("aggregate") was counted. One hundred cells were counted three times for each transfectant and the number of cells with the indicated mitochondrial morphology is shown as a percentage.

the tubulo-network structure. Taken together, the two Mfn isoforms or the GTPase domain mutants, when expressed in HeLa cells, induced clearly distinct mitochondrial morphologic changes, suggesting distinct functions of the two Mfn isoforms. The levels of exogenously expressed Mfn isoforms or mutants in HeLa cells were similar (see Fig. 2B). We also noticed using isoform-specific antibodies that endogenous Mfn1 and Mfn2 expression levels are similar in HeLa cells (data not shown). Therefore, we assume that the distinct mitochondrial morphologic changes observed after the expression of Mfn proteins are not affected by the endogenous levels of either isoform.

Mfn2^{K109T} Induces Mitochondrial Fragmentation and Is Clustered in the Junction between Adjacent Mitochondria—As described above, immunofluorescence microscopy revealed that expression of Mfn2^{K109T} induced mitochondrial fragmentation and the expressed protein accumulated in subdomains of the fragmented mitochondria as dot-like structures (see Fig. 2A, g–i, and magnified images in Fig. 3A, a–c), suggesting a dominant-negative effect on mitochondrial morphology. These properties were not previously recognized in GTPase-domain mutants of Fzo proteins or Mfn proteins. The endogenous form of Mfn1 colocalized with the expressed Mfn2^{K109T} (Fig. 3A, d–f), suggesting that the distribution of the endogenous components of the mitochondrial fusion machinery was affected by the exogenously expressed Mfn2^{K109T}, to cluster in subdomains of mitochondrial outer membranes, although the behavior of the endogenous Mfn2-isoform is not known.

Electron microscopic examination of HeLa cells expressing Mfn2^{K109T} revealed that smaller and circular mitochondria accumulated in the perinuclear regions (Fig. 3B, b and c) as compared with the structures in untransfected cells (Fig. 3B, a), structures that probably correspond to the fragmented mitochondria detected by immunofluorescent microscopy (see Fig. 3A). In magnified micrographs, the mitochondria were seem to be connected to neighboring mitochondria in several regions through electron-dense materials (Fig. 3B, c and d). Sometimes, there were mitochondria with budded tubular structures in the outer membrane (arrows in Fig. 3B, e). These results indicate that Mfn2^{K109T} expression induces the association of the mitochondrial outer membranes of neighboring mitochondria at restricted domains.

The localization of Mfn2^{K109T} was then analyzed by immuno-electronmicroscopy. Mfn2^{K109T} accumulated at the contact faces or tips between mitochondria, but few signals were detected in other areas of the outer membrane (Fig. 3B, f–h); 73% of gold particles on the mitochondria (of 432 particles counted) were localized on the contact domains. Sometimes, Mfn2^{K109T}-enriched membrane structures were observed in the areas intercalating between the contact regions of mitochondria (Fig. 3B, panel f). These structures appeared to be the dot-like structures observed by fluorescence microscopy (Fig. 3A, a–c) and the electron-dense regions of the outer membrane contacts observed by electron microscopy (Fig. 3B, c and d).

These results suggest that Mfn2^{K109T} expression arrests the mitochondrial fusion reaction at a certain stage, resulting in the accumulation of docked mitochondrial intermediates. Because endogenously expressed Mfn1 colocalizes with Mfn2^{K109T} in the dot-like structures (Fig. 3A, d–f), and the exogenously expressed Mfn1 and Mfn2 co-immunoprecipitate (see Fig. 5), the fusion-related components seem to be enriched in the closely apposed outer membrane regions.

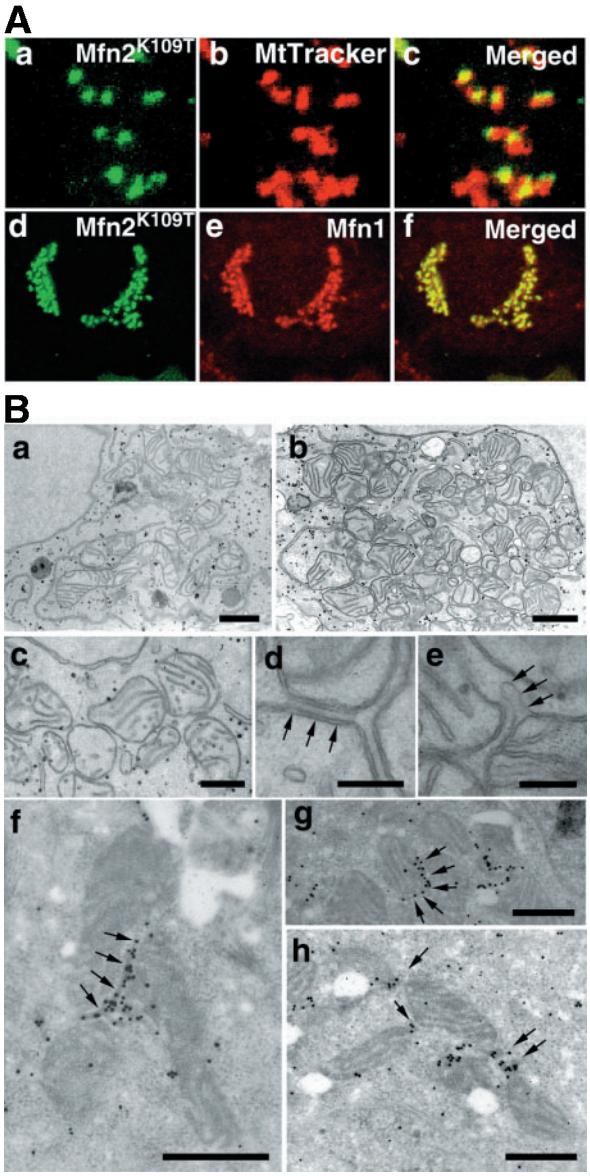

Fig. 3. **Expression of a GTPase mutant of rat Mfn2 inhibits mitochondrial fusion at intermediate stages.** (A) Cells expressing Mfn2^{K109T}-HA were co-stained with rabbit anti-HA (a) and MitoTracker (b), and the merged image is shown (c). Cells expressing Mfn2^{K109T}-HA were co-stained with mouse anti-HA (d) and rabbit anti-Mfn1 antibodies (e: for detection of endogenous Mfn1), and their merged image is shown (f). (B) Electron micrographs of HeLa cells expressing Mfn2^{K109T}-HA. HeLa cells expressing Mfn2^{K109T}-HA were cultured for 18 h, fixed, and prepared for electron microscopy as described in Materials and Methods. Mitochondrial structures of nontransfected (a) or transfected cells (b–h). (c–e) Higher magnification images of the mitochondria in the transfected cells. (f–h) Immuno-electron micrographs using rabbit anti-HA antibodies as described in "MATERIALS AND METHODS." Bars: 1 μm (a and b); 0.5 μm (c, f–h); 0.2 μm (d and e).

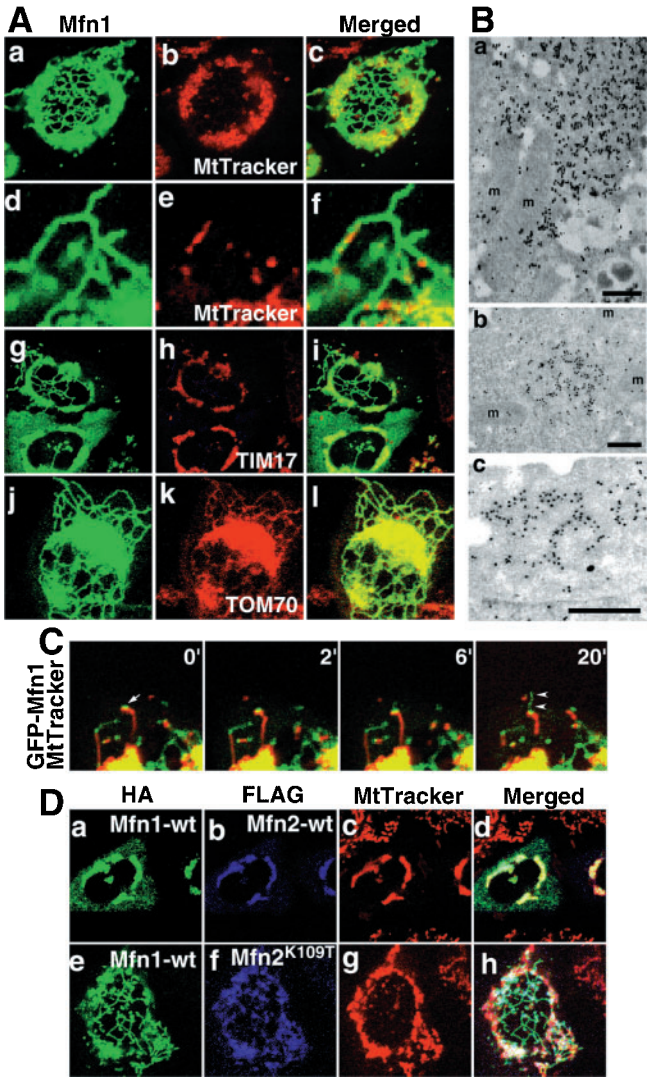

Fig. 4. **Tubulo-network structures of the outer membrane are induced by Mfn1.** (A) Mfn1-HA was transiently expressed in HeLa cells and cultured for 18 h. The cells were labeled with MitoTracker (b and e), then fixed and subjected to immunofluorescence microscopy using polyclonal anti-HA (a and d), monoclonal anti-HA (g and j), anti-Tim17 (h), and anti-Tom70 (k) antibodies. Merged images are shown (c, f, i, and l). (B) Electron micrographs of HeLa cells expressing Mfn1-FLAG. HeLa cells expressing Mfn1-FLAG were cultured for 18 h, fixed, and prepared for electron microscopy as described in Materials and Methods. m; mitochondrion, Bars; 0.5 μm. (C) Growth of GFP-Mfn1 containing tubular structures (green) as detected by time-lapse confocal microscopy. Mitochondria were labeled with MitoTracker (red). (D) Mfn1-HA was cotransfected with Mfn2-FLAG (a–d) or $Mfn2^{K109T}$-FLAG (e–h). The cells were stained with MitoTracker (c and g) and polyclonal anti-HA (a and e) or monoclonal anti-FLAG (b and f) antibodies, followed by visualization using FITC-conjugated anti-rabbit IgG, or Cy5-conjugated anti-mouse IgG. Merged images are shown in d and h.

Expression of Mfn1 Induces the Protrusion of Highly Connected Networks of the outer Membranes—We next analyzed more precisely the highly extended and connected tubulo-networks detected in Mfn1-transfected cells (see Fig. 2A, p–r). The structures containing Mfn1 co-stained with the outer membrane marker Tom70 (Fig. 4A, j–l), although they were counterstained only partly by MitoTracker or IgGs against the inner membrane marker Tim17 (Fig. 4A, a–f and g–I, and Fig. 4B). GFP-Mfn1, in which GFP is fused to the N-terminal of Mfn1, localized to the mitochondria and induced highly connected mitochondrial network structures when expressed in HeLa cells (data not shown). Time-lapse confocal microscopy also revealed that only the tubular structures containing the GFP-Mfn1 signal grew from the tips of the MitoTracker-positive tubules (Fig. 4C, arrow heads). We then examined the tubulo-network structures in HeLa cells expressing FLAG-tagged Mfn1 using immuno-electronmicroscopy with anti FLAG antibodies. Colloidal gold particles accumulated on the external surface of some structures clustered on the mitochondrial peripheri (Fig. 4B, a–c). They were not detectable in mock-transfected cells (data not shown). These structures probably represent the Mfn1-induced tubulo-network structures detected by fluorescence microscopy.

Although the membranous structures were not obvious with immuno-electronmicroscopy, we believe that they are membranous, because exogenously expressed Mfn1 was recovered in the membrane precipitates in the Triton X-100-soluble form (Fig. 2C). Together, these results suggest that the tubulo-network structures derive largely from the outer membranes and that Mfn1 with a functional GTPase domain is involved in the fusion or extension reactions of the outer membranes.

The Two Mfn Proteins Cooperate in Mitochondrial Morphogenesis—As described above, the expression of the two isoforms of rat Mfn had distinct effects on the mitochondrial morphology. Furthermore, mitochondrial fragmentation by $Mfn2^{K109T}$ or proliferation of the outer membrane induced by Mfn1 indicates that the two Mfn isoforms are involved in mitochondrial fusion events in mammalian cells. We, therefore, addressed whether these two isoforms function independently or cooperatively in the mitochondrial membrane fusion reaction by examining the effect of the co-expression of Mfn2 or $Mfn2^{K109T}$ on the Mfn1-induced tubulo-network structures.

As described, the tubulo-network structures were observed in ~30% of Mfn1-HA expressing cells (Fig. 2, A and D). These characteristic structures, however, were completely resolved by the co-expression of Mfn2-FLAG (in more than 100 cells examined; Fig. 4D, a–d), suggesting an interaction between the two Mfn proteins. On the other hand, co-expression of $Mfn2^{K109T}$ did not affect these structures (Fig. 4D, e–h), indicating that a functional GTPase domain in Mfn2 is required for recovery.

The physical interaction of the exogenously expressed isoforms in the mitochondrial membrane was then examined. HeLa cells cotransfected with Mfn2-FLAG and Mfn1-HA were solubilized with digitonin in the presence or absence of GTP or the unhydrolyzable analogue GTPγS and the supernatants were subjected to immunoprecipitation using antibodies against HA. Anti-HA antibody coprecipitated Mfn2-FLAG (Fig. 5A), although the precipitation efficiency was not affected by the presence of GTP or GTPγS. Immunoprecipitation also revealed a homotypic interaction between Mfn1-FLAG and Mfn1-HA or Mfn2-FLAG and Mfn2-HA (Fig. 5B), indicating that Mfn proteins can form homo-oligomeric complexes. As a control, the outer membrane protein Tom40 (Fig.

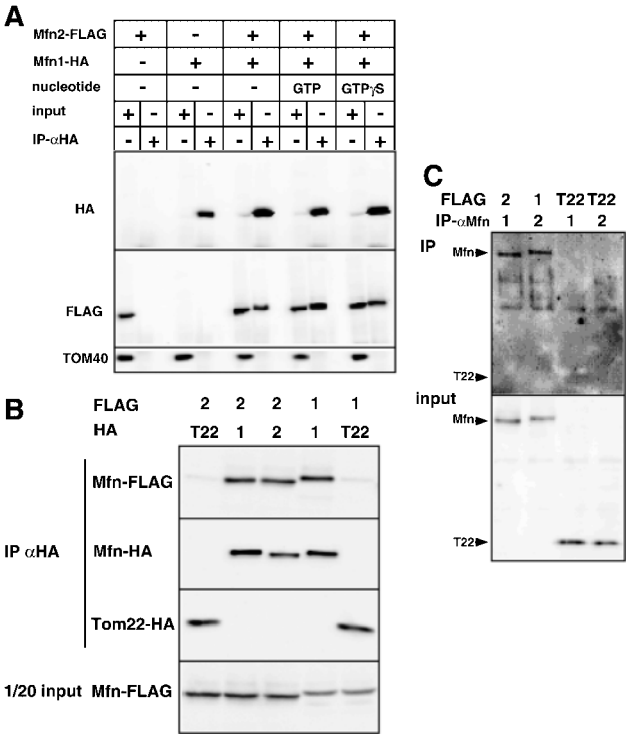

Fig. 5. **Immunoprecipitation of rat Mfn proteins expressed in HeLa cells.** (A) HeLa cells transfected with Mfn2-FLAG, Mfn1-HA, or both were solubilized with 1% digitonin in the presence or absence of 2 mM GTP or GTPγS. The supernatant fraction before immunoprecipitation (3.3% of total, "input"), or fractions immunoprecipitated with anti-HA polyclonal antibodies ("IP-αHA") were analyzed by immunoblotting using anti-FLAG monoclonal IgG, anti-HA monoclonal IgG, or anti-Tom40 polyclonal IgGs. (B) HeLa cells were transfected with HA- or FLAG-tagged Mfn2, Mfn1, or Tom22 in the indicated combinations. Immunoprecipitation was performed as in (A). (C) Complex formation of the endogenous Mfn proteins with the exogenously expressed FLAG-tagged Mfn proteins in HeLa cells. FLAG-tagged Mfn2, Mfn1 and Tom22 (T22) were transfected into HeLa cells, and immunoprecipitated using the indicated monospecific antibodies against Mfn proteins. Immunoprecipitated FLAG-tagged proteins ("IP") and whole cell extracts ("Input") were analyzed by immunoblotting using anti-FLAG antibodies.

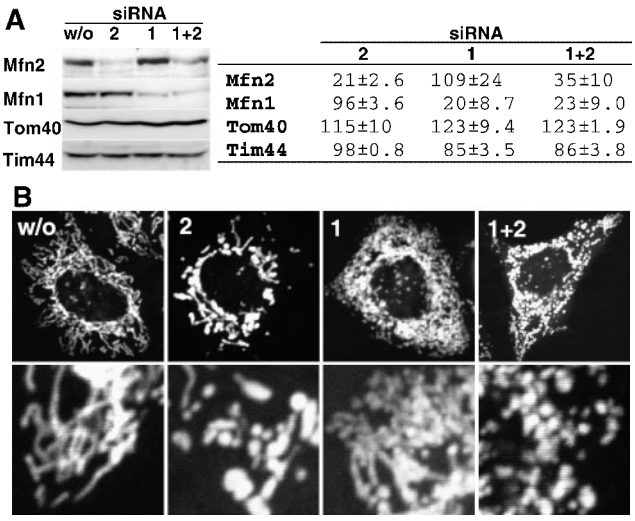

	siRNA 2	siRNA 1	siRNA 1+2
Mfn2	21±2.6	109±24	35±10
Mfn1	96±3.6	20±8.7	23±9.0
Tom40	115±10	123±9.4	123±1.9
Tim44	98±0.8	85±3.5	86±3.8

C

siRNA	normal	thick-tubule	shorter network	fragment
w/o	72.3±6.2	4.2±2.3	7.3±1.6	15.1±4.5
2	30.8±6.1	57.3±1.5	6.3±1.5	5.6±4.5
1	16.2±4.6	4.8±2.4	54.5±4.5	24.4±4.6
1+2	18.5±0.6	10.0±5.2	10.0±5.2	46.6±5.9

Fig. 6. **Depletion of Mfn isoforms in HeLa cells using RNAi.** HeLa cells were mock-transfected ("w/o") or transfected with the siRNA duplex for Mfn2 ("2"), Mfn1 ("1"), or a mixture of both ("1+2"). The cells were transfected twice with siRNAs at a 24-h interval. (A) Total cell extracts were analyzed by immunoblotting using the indicated antibodies. Intensity of each band was quantified and is shown in the table, with the intensity obtained for mock-transfection set at 100%. (B) The cells were stained with MitoTracker and analyzed by confocal laser-scanning microscopy. (C) Mitochondrial morphology. The numbers of siRNA-transfected HeLa cells with normal mitochondrial morphology ("normal"), thick mitochondria ("thick-tubule"), network structure of shorter mitochondria ("shorter network"), or fragmented mitochondria ("fragment") were counted. One hundred cells were counted three times. The number of cells with the indicated mitochondrial morphology is shown as a percentage.

5A) or HA-tagged outer membrane protein Tom22 (Fig. 5B) did not co-precipitate with Mfn1 or Mfn2. We then examined the interactions of the exogenously-expressed rat Mfn proteins with endogenous human Mfn proteins in HeLa cells. As shown in Fig. 5C, Mfn1-specific antibodies co-precipitated the exogenously-expressed rat Mfn2-FLAG, and Mfn2-specific antibodies co-precipitated Mfn1-FLAG. Thus, endogenous human Mfn proteins can form hetero-complexes with the exogenously expressed rat Mfn proteins in HeLa cells; this might have dominant effects on mitochondrial morphology (Figs. 2 and 3).

These results, in conjunction with the finding that the exogenously expressed $Mfn2^{K109T}$ colocalized with the endogenous Mfn1 (see Fig. 3A, d–f), indicate that the two Mfn isoforms function cooperatively in mitochondrial morphogenesis. The Mfn proteins might function as hetero-oligomeric and homo-oligomeric complexes in the outer membrane.

Two Mfn Proteins Are Essential for the Maintenance of Mitochondrial Morphology—As described above, the expression of either Mfn protein induced isoform-specific mitochondrial morphologic changes, suggesting that both isoforms function in the mitochondrial fusion reaction. To identify their function in the fusion process, we examined the effect of depletion of endogenous Mfn proteins on mitochondrial morphology using RNAi (*41*). Immunoblot analysis revealed that transfection of a 21-nucleotide siRNA duplex specific for one or both isoforms efficiently depleted one or both isoforms 48 h after the first transfection in HeLa cells (~70 to 80% depletion; Fig. 6A). On the other hand, the expressions of the unrelated mitochondrial proteins Tom40 and Tim44 were not significantly affected by the transfections, indicating that the RNAi reaction was specific for the Mfn isoforms. In approximately 70% of the mock-transfected cells, thin and filamentous network structures of mitochondria extending toward the cell peripheri were observed ("w/o" in Fig. 6, B and C). In marked contrast, the network structures decreased significantly (to ~30%) in the Mfn2-depleted cells. In addition, there were fewer branched, thick, and

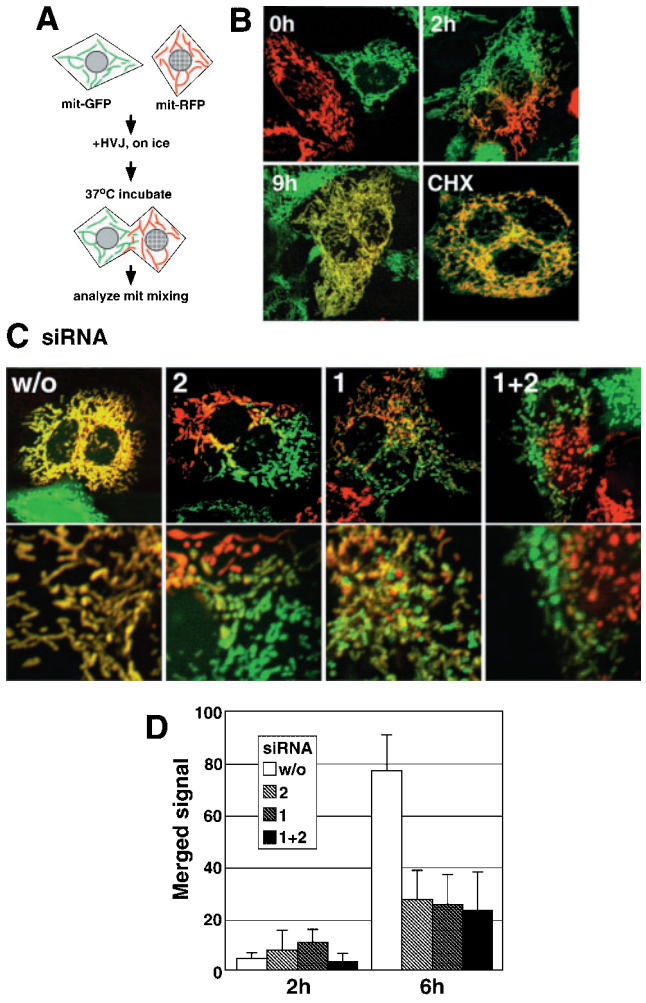

Fig. 7. **Mitochondrial fusion in HeLa cells and the effect of repression of Mfn isoforms.** (A) Schematic drawing of the mitochondrial fusion assay by HVJ-dependent cell fusion. (B) HeLa cells expressing Su9GFP and Su9RFP were co-cultured, and subjected to cell fusion as described in "MATERIALS AND METHODS." After cell fusion, the cells were cultured for 2 h or 9 h, and mitochondrial fluorescence proteins were analyzed by confocal laser microscopy. (CHX) 1 mM cycloheximide was added to the medium after the initiation of cell fusion and the cells were cultured for 9 h. (C) HeLa cells subjected to RNAi as in (B) were transfected with Su9GFP or Su9RGP. These cells were co-cultured and subjected to cell fusion. After 6 h incubation, the cells were analyzed for the localization of RFP and GFP fluorescence signals. (D) The merged fluorescence signals in fused cells were quantified. Fluorescence signals in the cytoplasm of 10 fused cells as described in (C) were analyzed by the MetaMorph colocalization measurement program.

shortened mitochondrial tubes, which accumulated around the nucleus but were sparse in the cytoplasm (~57%; "2" in Fig. 6B, and "thick-tubule" in Fig. 6C). These structures were rarely detected in mock-transfected cells. In approximately 50% of the Mfn1-depleted cells, the shortened mitochondrial structures with branches were dispersed throughout the cytoplasm ("1" in Fig. 6B, and "shorter network" in Fig. 6C). In cells subjected to the depletion of both isoforms, marked mitochondrial fragmentation occurred and the smaller vesicles accumulated throughout the cytoplasm ("1+2" in Fig. 6B, and "fragment" in Fig. 6C).

These results clearly indicate that both isoforms are essential for maintaining normal mitochondrial morphology. Furthermore, fragmentation of the mitochondrial networks into a distinct morphology induced by the depression of either isoform suggests that they are probably involved in distinct steps of mitochondrial fusion. The conclusions drawn from experiments of the exogenous expression of Mfn proteins were thus confirmed using a different approach.

Repression of Either Mfn Isoform Inhibits Mitochondrial Fusion as Demonstrated by HVJ-Mediated Cell Fusion—The data described above suggest that both Mfn proteins are involved in the mitochondrial fusion reaction. To address this point directly, we established an assay system for mitochondrial fusion (Fig. 7A). Two fluorescent proteins, GFP and DsRed (RFP), were fused, respectively, to the C-terminus of the mitochondrial matrix-targeting signal of *N. crassa* ATPase subunit 9 (Su9-GFP and Su9-RFP) at the cDNA level and expressed separately in HeLa cells. The cells harboring GFP- and RFP-labeled mitochondria were co-cultured in a dish, fused by HVJ (*36*) and the time-dependent mixing of the GFP and RFP signals was monitored by confocal microscopy (*42*). Both fluorescence signals were almost completely merged in the heterokaryon 9 h after the initiation of cell fusion (Fig. 7B), indicating that the mitochondrial contents of each cell were completely mixed by mitochondrial membrane fusion. Mixing of the fluorescence signals proceeded through frequent fusion and fission of the leading edges of the differentially labeled mitochondria (*42*). This mixing reaction was not inhibited by cycloheximide, indicating that *de novo* protein synthesis is not required for the mitochondrial fusion reaction and that the fluorescence signals do not represent newly synthesized Su9-GFP and Su9-RFP targeted to mitochondria after cell fusion (Fig. 7B).

Using this system, we analyzed the effects of the depletion of Mfn proteins. Cells expressing Su9-GFP or Su9-RFP were separately subjected to RNAi, co-cultured, and then fused by HVJ. In cells depleted of Mfn2, mitochondrial fusion reactions were blocked 6 h after fusion ("2" in Fig. 7C). Interestingly, the intermixing the GFP-labeled mitochondrial fragments and the RFP-labeled mitochondrial fragments was significantly inhibited in the heterokaryon. Depletion of Mfn1 also inhibited mitochondrial fusion. In this case, in contrast to Mfn2-depleted cells, intermixing of the fragmented or vesiculated mitochondria occurred in the heterokaryon, but their fusion was blocked ("1" in Fig. 7C). Thus, the depletion of Mfn1 or Mfn2 results in clearly distinct inhibition of the mitochondrial fusion reaction. Quantification of the merged fluorescence signal in the fused cells revealed that ~80% of total fluorescence signals were merged in mock-transfected cells 6 h after the initiation of cell fusion (Fig. 7D). In contrast, the fusion reaction was inhibited to 20 to 30% by the repression of either or both Mfn proteins (Fig. 7D). Thus, both Mfn isoforms are each involved distinctly in the mitochondrial fusion reaction.

DISCUSSION

It was previously reported that expression of either human Mfn1 or Mfn2 significantly affects mitochondrial morphology mainly through the fusion reaction (*29*, *30*, *43*). In the present study, we showed that the expression or repression of Mfn proteins led to isoform-specific mitochondrial morphologic changes, and both Mfn isoforms were essential for the mitochondrial fusion reaction.

The expression of rat Mfn2 in HeLa cells at moderate levels results in only marginal development of mitochondrial networks, although, as reported by Santel and Fuller (2001), Mfn2 overexpression induces mitochondrial clustering in the perinuclear region. Because similar clustering was also induced by the overexpression of mitochondrial outer membrane proteins, these mitochondrial aggregations seem to be partly due to the overproduction of outer membrane proteins, and, therefore, difficult to ascribe directly to the physiologic function of Mfn proteins (*29*). Instead, the GTPase domain mutant $Mfn2^{K109T}$, when expressed at lower levels in HeLa cells, induced fragmentation of the mitochondrial reticular structure and localized to the subdomains of mitochondria as dot-like structures. Of note, endogenous Mfn1 colocalized to the dot-like structures. These results suggest that endogenous Mfn proteins also accumulate on the dot-like structures, although the behavior of endogenous Mfn2 is not known. These unique structures have not been reported, however, for the GTPase domain-mutant of human Mfn2. Immuno-electronmicroscopy revealed that the expressed $Mfn2^{K109T}$ accumulates on the tips or faces of connecting mitochondria. These structures are probably the dot-like structures detected by fluorescence microscopy and correspond to the electron dense structures detected by electron microscopy between the outer membranes of closely apposed mitochondria. $Mfn2^{K109T}$ thus brings about a dominant-negative effect on the mitochondrial fusion reaction. It is possible that the regions in which these proteins accumulate are the microdomains of the mitochondrial outer membrane involved in the fusion reaction, where the fusion components are concentrated to form oligomeric structures after the arrest of the GTPase cycle of Mfn2.

The expression of wild-type Mfn1 in HeLa cells induced the protrusion of membranous structures to form highly branched tubular networks where the expressed Mfn1 was localized, whereas the GTPase domain mutant $Mfn1^{K88T}$ failed to induce such structures. Immuno-electronmicroscopy revealed Mfn1 signals aligned on some clustered structures, which might correspond to the tubular network structures detected under fluorescence microscopy. These characteristic structures contained the outer membrane protein Tom70, but were partly or less efficiently counterstained by MitoTracker or anti-Tim17 antibodies, suggesting that the structures were largely derived from the outer membranes. To our knowledge, these characteristic structures have not been reported previously and need to be characterized in detail. In this relation, co-expression of human Mfn2 with a dominant-negative mutant of dynamin-like protein ($Drp1^{K38A}$), which blocks the mitochondrial fission reaction, induces long filaments and network structures (*29*). These structures are co-immunostained with antibodies against the inner membrane marker COX1. Therefore, the structures induced by rat Mfn1 are distinct from those reported for Mfn2. Legros *et al*. (2002) also reported that the expression of human Mfn1 led to the appearance of highly elongated and branched mitochondria (*43*). Although the localization of the mitochondrial-subcompartment-marker proteins in these unique structures is not known, the structural features seem to be very similar to those induced by rat Mfn1 in the present study. Considering that mitochondrial fusion requires the concerted action of both outer and inner membranes, the overexpression of Mfn1 might disturb the concerted action between the two Mfn proteins, uncouple the fusion reaction of the outer membrane from that of the inner membrane, and enhance the outer membrane fusion or extension reactions.

Co-expression experiments provide some insight into the functional division of the two Mfn isoforms in mitochondrial fusion processes. The highly extended tubulo-network structures produced by high levels of Mfn1 expression were resolved by co-expression of Mfn2 with a functional GTPase domain, suggesting that both isoforms have distinct functions and cooperate in mitochondrial fusion processes. These results also suggest that a balance of the activity of both proteins is critical for maintaining a particular mitochondrial morphology or function.

These conclusions were supported by the RNAi experiments. Depletion of either of the isoforms induced mitochondrial fragmentation, although the effects were clearly distinct. Upon depletion of Mfn2, the typical network structures disappeared and thick, shortened, and less branched mitochondrial tubes formed around the nucleus. Depletion of Mfn1, on the other hand, induced fragmentation of the mitochondria into smaller structures with branches throughout the cytosol. Depletion of both isoforms enhanced fragmentation into small vesicles. These results indicate that both isoforms are required in the mitochondrial fusion reaction in mammalian systems, and that they are functionally distinct and irreplaceable. The assay for mitochondrial fusion in the heterokaryons produced by HVJ in conjunction with the RNAi clearly indicates that both Mfn proteins are involved in the fusion reaction. Because repression of either of the isoforms strongly inhibited the fusion reaction, the two isoforms do not have functional redundancy but seem to function cooperatively in the fusion reaction. In this relation, Chen *et al*. (*46*) have recently reported, based on the results of experiments with Mfn-knockout mice, that two Mfn proteins are required for mitochondrial fusion and morphogenesis, results that largely agree with those in the present report. They also reported that both Mfn proteins are essential for embryonic development. These results, together with the difference in the expression levels of these isoforms in rat tissues, suggest that the relative content of Mfn1 and Mfn2 determines tissue-specific mitochondrial morphology, dynamics, or functions in cooperation with other factors such as Drp1 and OPA1.

Mitochondria exhibit a dispersed distribution in Mfn1-repressed HeLa cells and, during the fusion of Mfn1-repressed cells, mitochondrial intermixing proceeded normally, although fusion was inhibited (see Figs. 6B and 7C). In contrast, mitochondrial fusion was strongly

arrested in Mfn2-repressed cells at the step of mitochondrial intermixing (see Fig. 7C). These results suggest that Mfn proteins are also involved in the organization or positioning of mitochondria within cells; thus the balance of expression between Mfn1 and Mfn2 in tissues might reflect tissue-specific mitochondrial morphology.

Hemagglutinating Virus of Japan (HVJ, Sendai Virus) was a generous gift from Dr. Y. Yoneda (Osaka University). This work was supported by grants from the Ministry of Education, Science, and Culture of Japan, the Human Frontier Science Program, and Core Research from Evolutional Science and Technology to K.M.

REFERENCES

1. Hermann, G.J. and Shaw, J.M. (1998) Mitochondrial dynamics in yeast. *Annu. Rev. Cell. Dev. Biol.* **14**, 265–303
2. Yaffe, M.P. (1999) The machinery of mitochondrial inheritance and behavior. *Science* **283**, 1493–1497
3. Jensen, R.E., Hobbs, A.E., Cerveny, K.L., and Sesaki, H. (2000) Yeast mitochondrial dynamics: fusion, division, segregation, and shape. *Microsc. Res. Tech.* **51**, 573–583
4. McConnell, S.J. and Yaffe, M.P. (1993) Intermediate filament formation by a yeast protein essential for organelle inheritance. *Science* **260**, 687–689
5. Sesaki, H. and Jensen, R.E. (1999) Division versus fusion: Dnm1p and Fzo1p antagonistically regulate mitochondrial shape. *J. Cell Biol.* **147**, 699–706
6. Shaw, J.M. and Nunnari, J. (2002) Mitochondrial dynamics and division in budding yeast. *Trends Cell Biol.* **12**, 178–184
7. Otsuga, D., Keegan, B.R., Brisch, E., Thatcher, J.W., Hermann, G.J., Bleazard, W., and Shaw, J.M. (1998) The dynamin-related GTPase, Dnm1p, controls mitochondrial morphology in yeast. *J. Cell Biol.* **143**, 333–349
8. Bleazard, W., McCaffery, J.M., King, E.J., Bale, S., Mozdy, A., Tieu, Q., Nunnari, J., and Shaw, J.M. (1999) The dynamin-related GTPase Dnm1 regulates mitochondrial fission in yeast. *Nat. Cell Biol.* **1**, 298–304
9. Jones, B.A. and Fangman, W.L. (1992) Mitochondrial DNA maintenance in yeast requires a protein containing a region related to the GTP-binding domain of dynamin. *Genes Dev.* **6**, 380–389
10. Guan, K., Farh, L., Marshall, T.K., and Deschenes, R.J. (1993) Normal mitochondrial structure and genome maintenance in yeast requires the dynamin-like product of the MGM1 gene. *Curr. Genet.* **24**, 141–148
11. Shepard, K.A. and Yaffe, M.P. (1999) The yeast dynamin-like protein, Mgm1p, functions on the mitochondrial outer membrane to mediate mitochondrial inheritance. *J. Cell Biol.* **144**, 711–720
12. Pelloquin, L., Belenguer, P., Menon, Y., Gas, N., and Ducommun, B. (1999) Fission yeast Msp1 is a mitochondrial dynamin-related protein. *J. Cell Sci.* **112**, 4151–4161
13. Wong, E.D., Wagner, J.A., Gorsich, S.W., McCaffery, J.M., Shaw, J.M., and Nunnari, J. (2000) The dynamin-related GTPase, Mgm1p, is an intermembrane space protein required for maintenance of fusion competent mitochondria. *J. Cell Biol.* **151**, 341–352.
14. Hales, K.G. and Fuller, M.T. (1997) Developmentally regulated mitochondrial fusion mediated by a conserved, novel, predicted GTPase. *Cell* **90**, 121–129
15. Hermann, G.J., Thatcher, J.W., Mills, J.P., Hales, K.G., Fuller, M.T., Nunnari, J., and Shaw, J.M. (1998) Mitochondrial fusion in yeast requires the transmembrane GTPase Fzo1p. *J. Cell Biol.* **143**, 359–373
16. Rapaport, D., Brunner, M., Neupert, W., and Westermann, B. (1998) Fzo1p is a mitochondrial outer membrane protein essential for the biogenesis of functional mitochondria in Saccharomyces cerevisiae. *J. Biol. Chem.* **273**, 20150–20155
17. Fritz, S., Rapaport, D., Klanner, E., Neupert, W., and Westermann, B. (2001) Connection of the mitochondrial outer and inner membranes by Fzo1 is critical for organellar fusion. *J. Cell Biol.* **152**, 683–692
18. Shin, H.W., Shinotsuka, C., Torii, S., Murakami, K., and Nakayama, K. (1997) Identification and subcellular localization of a novel mammalian dynamin-related protein homologous to yeast Vps1p and Dnm1p. *J. Biochem. (Tokyo)* **122**, 525–530
19. Imoto, M., Tachibana, I., and Urrutia, R. (1998) Identification and functional characterization of a novel human protein highly related to the yeast dynamin-like GTPase Vps1p. *J. Cell Sci.* **111**, 1341–1349
20. Kamimoto, T., Nagai, Y., Onogi, H., Muro, Y., Wakabayashi, T., and Hagiwara, M. (1998) Dymple, a novel dynamin-like high molecular weight GTPase lacking a proline-rich carboxyl-terminal domain in mammalian cells. *J. Biol. Chem.* **273**, 1044–1051
21. Yoon, Y., Pitts, K.R., Dahan, S., and McNiven, M.A. (1998) A novel dynamin-like protein associates with cytoplasmic vesicles and tubules of the endoplasmic reticulum in mammalian cells. *J. Cell Biol.* **140**, 779–793
22. Smirnova, E., Shurland, D.L., Ryazantsev, S.N., and van der Bliek, A.M. (1998) A human dynamin-related protein controls the distribution of mitochondria. *J. Cell Biol.* **143**, 351–358
23. Pitts, K.R., Yoon, Y., Krueger, E.W., and McNiven, M.A. (1999) The dynamin-like protein DLP1 is essential for normal distribution and morphology of the endoplasmic reticulum and mitochondria in mammalian cells. *Mol. Biol. Cell* **10**, 4403–4417
24. Smirnova, E., Griparic, L., Shurland, D.L., and van Der Bliek, A.M. (2001) Dynamin-related protein drp1 is required for mitochondrial division in mammalian cells. *Mol. Biol. Cell* **12**, 2245–2256
25. Yoon, Y., Pitts, K.R., and McNiven, M.A. (2001) Mammalian dynamin-like protein dlp1 tubulates membranes. *Mol. Biol. Cell* **12**, 2894–2905
26. Frank, S., Gaume, B., Bergmann-Leitner, E., Leitner, W., Robert, E., Catez, F., Smith, C., and Youle, R. (2001) The role of dynamin-related protein **1**, a mediator of mitochondrial fission, in apoptosis. *Dev. Cell* **4**, 515–525
27. Alexander, C., Votruba, M., Pesch, U.E., Thiselton, D.L., Mayer, S., Moore, A., Rodriguez, M., Kellner, U., Leo-Kottler, B., Auburger, G., Bhattacharya, S.S., and Wissinger, B. (2000) OPA1, encoding a dynamin-related GTPase, is mutated in autosomal dominant optic atrophy linked to chromosome 3q28. *Nat. Genet.* **26**, 211–215
28. Delettre, C., Lenaers, G., Griffoin, J.M., Gigarel, N., Lorenzo, C., Belenguer, P., Pelloquin, L., Grosgeorge, J., Turc-Carel, C., Perret, E., Astarie-Dequeker, C., Lasquellec, L., Arnaud, B., Ducommun, B., Kaplan, J., and Hamel, C.P. (2000) Nuclear gene OPA1, encoding a mitochondrial dynamin-related protein, is mutated in dominant optic atrophy. *Nat. Genet.* **26**, 207–210
29. Santel, A. and Fuller, M.T. (2001) Control of mitochondrial morphology by a human mitofusin. *J. Cell Sci.* **114**, 867–874
30. Rojo, M., Legros, F., Chateau, D., and Lombes, A. (2002) Membrane topology and mitochondrial targeting of mitofusins, ubiquitous mammalian homologs of the transmembrane GTPase Fzo. *J. Cell Sci.* **115**, 1663–1674
31. Mihara, K. (1990) Structure and regulation of rat liver microsomal stearoyl-CoA desaturase gene. *J. Biochem. (Tokyo)* **108**, 1022–1029
32. Suzuki, H., Okazawa, Y., Komiya, T., Saeki, K., Mekada, E., Kitada, S., Ito, A., and Mihara, K. (2000) Characterization of rat TOM40, a central component of the preprotein translocase of the mitochondrial outer membrane. *J. Biol. Chem.* **275**, 37930–37936
33. Suzuki, H., Maeda, M., and Mihara, K. (2002) Characterization of rat TOM70 as a receptor of the preprotein translocase of the mitochondrial outer membrane. *J. Cell Sci.* **115**, 1895–1905
34. Ishihara, N. and Mihara, K. (1998) Identification of the protein import components of the rat mitochondrial inner membrane,

rTIM17, rTIM23, and rTIM44. *J. Biochem. (Tokyo)* **123**, 722–732
35. Saeki, K., Suzuki, H., Tsuneoka, M., Maeda, M., Iwamoto, R., Hasuwa, H., Shida, S., Takahashi, T., Sakaguchi, M., Endo, T., Miura, Y., Mekada, E., and Mihara, K. (2000) Identification of mammalian TOM22 as a subunit of the preprotein translocase of the mitochondrial outer membrane. *J. Biol. Chem.* **275**, 31996–32002
36. Kose, S., Imamoto, N., Tachibana, T., Yoshida, M., and Yoneda, Y. (1999) beta-subunit of nuclear pore-targeting complex (importin-beta) can be exported from the nucleus in a Ran-independent manner. *J. Biol. Chem.* **274**, 3946–3952
37. Ukaji, K., Ariyoshi, N., Sakaguchi, M., Hamasaki, N., and Mihara, K. (2002) Membrane topogenesis of the three amino-terminal transmembrane segments of Glucose-6-phosphatase on endoplasmic reticulum. *Biochem. Biophys. Res. Commun.* **292**, 153–160
38. Ungermann, C., Neupert, W., and Cyr, D.M. (1994) The role of Hsp70 in conferring unidirectionality on protein translocation into mitochondria. *Science* **266**, 1250–1253
39. Ishihara, N., Yamashina, S., Sakaguchi, M., Mihara, K., and Omura, T. (1995) Malfolded cytochrome P-450(M1) localized in unusual membrane structures of the endoplasmic reticulum in cultured animal cells. *J. Biochem. (Tokyo)* **118**, 397–404
40. Yokota, S., Kamijo, K., and Oda, T. (2000) Aggregate formation and degradation of overexpressed wild-type and mutant urate oxidase proteins. Quality control of organelle-destined proteins by endoplasmic reticulum. *Histochem. Cell Biol.* **114**, 433–446
41. Elbashir, S.M., Harborth, J., Lendeckel, W., Yalcin, A., Weber, K., and Tuschl, T. (2001) Duplexes of 21-nucleotide RNAs mediate RNA interference in cultured mammalian cells. *Nature* **411**, 494–498
42. Ishihara, N., Jofuku, A., Eura, Y., and Mihara, K. (2003) Regulation of mitochondrial morphology by membrane potential and DRP1-dependent division and FZO1-dependent fusion reaction in mammalian cells. *Biochem. Biophys. Res. Commun.* **301**, 891–898
43. Legros, F., Lombes, A., Frachon, P., and Rojo, M. (2002) Mitochondrial fusion in human cells is efficient, requires the inner membrane potential, and is mediated by mitofusins. *Mol. Biol. Cell* **13**, 4343–4354
44. Kanaji, S., Iwahashi, J., Kida, Y., Sakaguchi, M., and Mihara, K. (2000) Characterization of the signal that directs Tom20 to the mitochondrial outer membrane. *J. Cell Biol.* **151**, 277–288
45. Yano, M., Kanazawa, M., Terada, K., Namchai, C., Yamaizumi, M., Hanson, B., Hoogenraad, N., and Mori, M. (1997) Visualization of mitochondrial protein import in cultured mammalian cells with green fluorescent protein and effects of overexpression of the human import receptor Tom20. *J. Biol. Chem.* **272**, 8459–8465
46. Chen, H., Detmer, S., Ewald, A., Griffin, E., Fraser, S., and Chan, D. (2003) Mitofusins Mfn1 and Mfn2 coordinately regulate mitochondrial fusion and are essential for embryonic development. *J. Cell Biol.* **160**, 189–200